Lamellar Diblock Copolymer Thin Films Investigated by Tapping Mode Atomic Force Microscopy: Molar-Mass Dependence of Surface Ordering

Peter Busch,*,† Dorthe Posselt,‡ Detlef-M. Smilgies,§ Bernd Rheinländer,† Friedrich Kremer,† and Christine M. Papadakis†

Faculty of Physics and Earth Sciences, University of Leipzig, Linnéstr. 5, D-04103 Leipzig, Germany; Department of Mathematics and Physics (IMFUFA), Roskilde University, P.O. Box 260, DK-4000 Roskilde, Denmark; and Cornell High Energy Synchrotron Source (CHESS), Wilson Laboratory, Cornell University, Ithaca, New York 14853

Received March 25, 2003; Revised Manuscript Received September 3, 2003

ABSTRACT: Using tapping mode atomic force microscopy, we studied the influence of molar mass (13.9−183 kg/mol) on the lamellar orientation at the surface of thin films of symmetric polystyrene−polybutadiene diblock copolymers prepared via spin-coating and by slow solvent-casting. The ratio between film thickness and lamellar thickness was varied between 0.5 and 10. Whereas for film thicknesses between 1 and 10 times the lamellar thickness, a lamellar orientation parallel to the film surface is preferred for low molar masses (below ∼55 kg/mol), high molar mass samples (above ∼90 kg/mol) rather form lamellae oriented perpendicular to the surface. For film thicknesses equal to the lamellar thickness, the films do not exhibit any texture, whereas for film thicknesses equal to half the lamellar thickness, a weak surface structure could be observed. This is consistent with symmetric wetting, i.e., the same block adsorbs at both film interfaces, but their selectivity is only weak. Thus, entropic contributions like chain stretching along a wall and the enrichment of free chain ends at the interface become important, and both parallel and perpendicular orientations of lamellae in thin films can occur.

Introduction

Because of their ability to self-assemble into highly regular structures with mesoscopic length scales, diblock copolymers present an interesting class of materials for thin film technology.[1,2] In the bulk, the interplay of the incompatibility between the different blocks and the fact that they are covalently linked on a molecular level gives rise to a variety of ordered microdomain structures in thermal equilibrium (e.g., refs 3−5). For equal volume fractions of the two blocks (i.e., symmetric diblock copolymers), either disordered or lamellar structures are formed, depending on the product of the Flory−Huggins interaction parameter χ and the overall degree of polymerization N.[5] To minimize the interfacial area between A and B parts of the lamellae, the chains are stretched normal to the lamellar interfaces,[6] thus leading to a scaling behavior $D_{lam} \propto N^{\alpha}$ of the bulk equilibrium lamellar thickness, D_{lam} (which comprises both an A and a B layer), with N. Values for α of 0.64−0.67 have been predicted for the strong-segregation limit (large values of χN),[7,8] and a value of 0.61 ± 0.02 has been found experimentally for polystyrene−polybutadiene (PS−PB) for $\chi N = 30-100$.[9]

For block copolymer thin films with film thicknesses of the order of a few times the lamellar thickness, the lamellar orientation is affected by a number of additional parameters, such as the interfacial energy of each block at both the substrate/film and the film/air interfaces and the reduced film thickness D_{red}, which is the ratio of the film thickness D_{film} and D_{lam}.[10]

We present a study of the lamellar orientation in thin films of symmetric PS−PB diblock copolymers on silicon substrates terminated with a native silicon oxide layer (Si/SiO_x). A wide range of molar masses ($\bar{M}_n = 13.9-183$ kg/mol) and reduced film thicknesses (D_{red} between 0.5 and 10) were investigated. The surface structures of these films were determined using tapping mode atomic force microscopy (TMAFM). Before describing the results obtained, we give an overview of previous experimental and theoretical findings on lamellar diblock copolymer thin films.

A well-studied system is thin films of polystyrene−poly(methyl methacrylate) (PS−PMMA) on Si/SiO_x substrates, where it has repeatedly been found that for $D_{red} \geq 0.5$ the lamellae are oriented parallel to the substrate.[11−15] While the strong interaction of the polar PMMA block with the polar SiO_x layer leads to the coverage of the substrate by the PMMA block, the lower surface tension of PS leads to segregation of PS to the free film/air surface. In this case (so-called antisymmetric wetting),[10] a homogeneous film can only be obtained for film thicknesses $D_{red} = m + {}^1/_2$, where m is an integer. For film thicknesses different from these values, an incomplete layer with islands or holes is formed at the free film surface with step heights similar to D_{lam}.[12,16−20] The high affinity of PMMA toward the SiO_x substrate compared to the one of PS could be demonstrated in several studies:[11,21] It was shown that, even above the order-to-disorder transition temperature, where the two blocks become miscible in the bulk, an enrichment of PMMA at the film interfaces (Si/SiO_x) takes place in thin film geometry, which is consistent with theory.[22]

For thin block copolymer films between two hard walls, the formation of islands or holes is prohibited. Nonetheless, the parallel orientation is maintained for PS−PMMA, even for any noninteger value of m, as long as the walls are selective enough to the PMMA block.[23] In this case, the high affinity of the PMMA block to the

* To whom correspondence should be addressed: e-mail pbusch@rz.uni-leipzig.de.
† University of Leipzig.
‡ Roskilde University.
§ Cornell University.

10.1021/ma034375r CCC: $25.00
Published on Web 10/15/2003

walls is so strong as to compensate the incommensurability between D_{film} and D_{lam} by a periodic contraction and expansion of the lamellae, i.e., by deviations from D_{lam}.

In ultrathin films of PS−PMMA ($D_{red} < 0.5$), various structures with parallel orientation as well as hybrid structures of parallel and laterally structured layers have been found as a function of D_{red} and the ratio of selectivities of the film interfaces. A detailed description of these morphologies has been given in a recent review.[10]

In PS−PB diblock copolymers, both blocks are rather nonpolar; i.e., the substrate is close to nonselective. Thus, the tendency of preferential adsorption of one of the two blocks to the (polar) SiO_x layer of a silicon substrate is much lower than for the PS−PMMA system, and other factors may come into play and determine the lamellar orientation as shown in the work presented here.

Only very thick solvent-cast films ($D_{red} \approx 10^3-10^6$) of lamellar PS−PB or PS−polyisoprene (PS−PI, PI being chemically very similar to PB) have been studied, and very different findings have been made.[24−26] By means of cross-sectional transmission electron microscopy (TEM) on films of lamellar PS−PI with $\bar{M}_n = 524$ kg/mol, it has been found that the parallel orientation is the dominant orientation, but also areas with a perpendicular orientation are present.[24] For films of PS−PB samples with $\bar{M}_n = 90$ kg/mol, Schwark et al. found by combining TEM with AFM that the lamellae are tilted with respect to the film surface.[25] Turturro et al. showed that the orientation is affected by the evaporation time of the solvent.[26] Whereas a short evaporation time (over 3 days) leads to a perpendicular orientation for low (21 kg/mol) and high (122 kg/mol) molar mass PS−PI, the parallel orientation was found for both molar masses, when the solvent was evaporated slowly (over 3 weeks). A similar effect of the evaporation time on the orientation of the mesostructure was observed in thin films ($D_{red} < 10$) of cylindrical PS−PB−PS triblock copolymers.[27,28]

In theoretical studies,[29−33] the key factors governing the thin film morphology in thin films between hard walls have been identified: Turner[29] and Walton et al.[30] have found that the parallel lamellar orientation is stable for $D_{red} = m$ if both surfaces are selective to the same block (symmetric wetting) or for $D_{red} = m + 1/2$ if the surfaces are selective to different blocks (antisymmetric wetting), respectively. For other values of D_{red}, the entropic penalty related to the perturbation of the lamellar thicknesses can be overcome by forming the perpendicular orientation, where the lamellae can maintain their bulk equilibrium lamellar thickness.[30,34] Thus, an alternating parallel and perpendicular orientation is predicted as D_{red} is varied. Only for D_{red} large enough, the parallel orientation becomes stable even if D_{film} and D_{lam} are not commensurable, since in this case chain deformation is distributed over many layers. This limiting value for D_{red} depends only on the selectivity of the walls to the blocks and not, for instance, on molar mass.[30]

Pickett et al. considered two additional contributions determining the lamellar orientation near a wall, in particular for the case of a weakly selective wall.[35,36] They took into account that the chains in the microphase-separated state are under tension because they are stretched normal to the lamellar interface. If these chains come into contact with a wall, the wall lowers their tension by inducing a nematic ordering,[35,36] which forces the chains to lie preferentially parallel to the wall. This leads to a perpendicular orientation of the lamellae with respect to the film interfaces. The second argument arises from the enrichment of chain end segments near a wall which favors the parallel orientation. Similar results were obtained in Monte Carlo simulations by Sommer et al.: The lamellae are perpendicular to perfectly nonselective walls.[37] Experimentally, this prediction was confirmed by creating nonselective walls for PS−PMMA diblock copolymers by coating the substrate with PS−PMMA random copolymers.[15,38−41]

Theoretical studies of thin, supported films, i.e., films with a hard wall interface and a free film surface, are scarce and deal with ultrathin films only.[10,32,42] Depending on the conditions, both parallel and perpendicular lamellae as well as hybrid structures have been predicted.

In the present work, we have studied the surface structure of thin films of nine symmetric PS−PB diblock copolymer samples with different molar masses. The samples were prepared by spin-coating from toluene solution onto silicon substrates terminated with a native silicon oxide layer. To determine the influence of the overall block copolymer molar mass and of the reduced film thickness, these parameters were varied in a wide range ($\bar{M}_n = 13.9-183$ kg/mol and $D_{red} = 0.5-10$). Increasing the molar mass has several implications: (i) D_{lam} increases and (ii) χN increases, which leads to stronger segregation (thus narrower lamellar interfaces) and to stronger chain stretching. To determine the influence of the solvent evaporation time and to test whether the results obtained by spin-coating can be reproduced, a few samples were prepared by solvent-casting as well.

The present publication is an account of our AFM studies of the surface topography of thin block copolymer films. In a second forthcoming publication,[43] we will present an investigation of the same films with grazing-incidence small-angle X-ray scattering (GISAXS) to elucidate the inner film structure. The results are in good agreement with the results presented here but give additional information about the lamellar orientation inside the films.

The paper is organized as follows: First, results from TMAFM on a series of spin-coated films with $D_{red} = 2.4-3.2$ are presented, and it will be shown that the lamellar orientation depends on molar mass in a characteristic way. Then, we show that this behavior is also found for larger values of D_{red}. Next, we discuss films with $D_{red} < 1$. The effect of the solvent evaporation time is addressed, and finally, the results are discussed in terms of the enthalpic and entropic contributions to the free energy of the films.

Experimental Section

The polystyrene−polybutadiene (PS−PB) diblock copolymers used in this study were synthesized by anionic polymerization.[44] All samples have a PB volume fraction of 0.49 ± 0.01.[9,45] The polymer characteristics are compiled in Table 1. The χ parameter is $\chi = A/T + B$ with $A = 21.6 \pm 2.1$ K and $B = -0.019 \pm 0.005$.[45] The glass transition temperature of the homopolymer polystyrene depends on molar mass according to T_g [K] $= 373 - 1.0 \times 10^5/M_n$ [g/mol].[46] For the PS blocks of the samples studied in this work, T_g values between ~90 and 100 °C are thus expected. Differential scanning calorimetry

Table 1. Characteristics of the Diblock Copolymers Used[a]

$\bar{M}_n$[b] [kg/mol]	N[c]	D_{lam}[d] [Å]	T_{ODT}[e] [°C]
13.9	236	138 ± 3	71 ± 1
18.3	310	160 ± 3	130 ± 2
22.1	374	189 ± 1	181 ± 2
22.6	383	197 ± 4	204 ± 1
54.5	921	413 ± 3	*f*
69.9	1182	462 ± 4	*f*
91.9	1555	528 ± 4	*f*
148	2511	752 ± 4	*f*
183	3090	839 ± 13	*f*

[a] All values were taken from refs 9 and 45. D_{lam} at room temperature is expected to be a few percent larger than at 150 °C.[45] [b] Overall copolymer molar mass. [c] Corresponding degree of polymerization. [d] Bulk lamellar thickness as measured by small-angle X-ray scattering at 150 °C. [e] Order-to-disorder transition temperatures. [f] Above the highest accessible temperature.

measurements on the PS−PB diblock copolymers gave values of 76 and 102 °C for $\bar{M}_n$ = 22.1 and 54.5 kg/mol.[45] The T_g of PB is below −80 °C.[46] The values for the surface tensions of PS and PB found in the literature scatter considerably.[26,47−49] However, recently measured values[26] are $\gamma_C^{PS} = 33$ mN/m and $\gamma_C^{PB} = 28$ mN/m for 7% 1,2-addition of PB, corresponding to the present case.[9,45]

Spin-coated films were prepared on Si(111) wafers terminated with a native silicon oxide layer (Silchem Handelsgesellschaft mbH). The wafers were cleaned by treating them with a detergent solution at 60 °C for 3 days and by rinsing them with water and toluene (purchased from Aldrich, 99.5+% purity, A.C.S. spectrophotometric grade). The polymers were dissolved in toluene together with ∼1% w/w (relative to the polymer mass) antioxidant (Irganox 1010 from CIBA) to prevent cross-linking of the PB blocks during further treatment. Solutions with polymer concentrations between 0.1% and 7% w/w were poured onto the Si wafers until these were completely wet, and then the wafers were rotated at 3000 rpm for 30 s. The solutions are in the disordered state and not lamellar.[50] To remove traces of solvent and to drive the films toward equilibrium, samples with $\bar{M}_n \geq 54.5$ kg/mol were kept in high vacuum (∼10^{-5} mbar) at a temperature of 150 °C for up to 3 days, i.e., well above both glass transition temperatures but still in the lamellar state. AFM images of as-cast and of annealed samples did not show any significant differences with respect to the texture (lamellae or terraces). Longer annealing times and higher annealing temperatures were avoided because of the thermal instability of the PB block. Films with $\bar{M}_n \leq 22.6$ kg/mol were dried under high vacuum at room temperature to avoid dewetting at high temperatures.[51]

The film thicknesses were determined using standard spectroscopic ellipsometry.[52] For the measurements, a rotating-analyzer spectral ellipsometer of the type V.A.S.E. (J.A.Woollam Co., Inc.) was applied. The spectra in the ellipsometric parameters Ψ and Δ were recorded at the spin-coated film samples on illuminated sample areas of 5 × 8 mm² at room temperature in the energy range 1.5−4.3 eV with a spectral resolution of 25 meV at angles of incidence of 60° and 67°. For the determination of the film thicknesses, the optical properties of the samples were modeled assuming a three-layer structure: (i) the undoped Si substrate, (ii) the nonabsorbing SiO_2 layer, and (iii) the nonabsorbing PS−PB layer. For the latter one, a possible thickness nonuniformity was taken into consideration. For Si and SiO_2, updated optical constants involved in the J.A.Woollam ellipsometer were applied. The refractive index of the PS−PB films was modeled by a Bruggeman type effective-medium approximation on the basis of data evaluated in the following manner: In all cases, the spectra of the refractive index were described assuming a Cauchy approximation: $n = A + B/\lambda^2$ (with the wavelength λ in units of micrometers). For PS, the value $A = 1.5191$ is taken from a fit to refractive index data given in the literature.[53] The dispersion term $B = 6.012 \pm 0.001$ μm² was determined experimentally on a single PS film by spectroscopic ellipsometry. For PB, the values $A = 1.529 \pm 1.006$ and $B = 0.078 \pm 0.006$ μm² and the film thicknesses were found by a simultaneous multisample fit including four samples with PS−PB films with thicknesses in the range 2200−2500 Å. For the effective-medium approximation, equal fractions of PS and PB were assumed. For the PS component, the refractive index data named before were applied. The thicknesses of the spin-coated films, D_{film}, were deduced on the basis of the layer model described. For nearly the half number of samples, no thickness nonuniformity could be detected over the light-illuminated area. In the other cases, the thickness nonuniformity amounts to 4−8%. The error of the averaged thickness values is typically ±0.5% or ±5 Å and enters the D_{red} values.

Additionally, two samples (18.3 and 183 kg/mol) were prepared by slow solvent-casting: Silicon wafers were wet with the polymer solutions with a polymer concentration of 0.2% w/w and placed in a closed Petri dish. The solvent (toluene) was left to evaporate for 3 days. As the films obtained in this way have inhomogeneous film thicknesses, the local film thicknesses at the positions, where the surface structures were studied, were determined by scribing grooves into the polymer films and by measuring their depth using AFM.

The film surfaces were investigated by TMAFM. In tapping mode, the scanning tip vibrates close to its resonance frequency. While scanning, viscoelastic interactions between tip and polymer surface lead to a damping and a phase shift of the vibration of the cantilever as compared to the vibration without interaction. Images recorded at constant damping are referred to as height images. Simultaneously with the height images, the phase shifts are recorded, which are sensitive to the viscoelastic properties of the film surface and provide thus contrast between different materials. We used a Dimension 3000 scanning probe microscope with a Nanoscope IIIa controller (Digital Instruments Inc., Santa Barbara, CA) in combination with a phase extender box. We used POINTPROBE Silicon-SPM sensors, type NCL from Nanosensors, with a typical resonance frequency of around 190 kHz. The set-point ratio r_{sp}, i.e., the ratio between the set-point amplitude A_{sp} and the free vibrational amplitude A_0 (the lowest amplitude when tip and sample are not in contact, just above the surface), was chosen to be 0.6−0.7. The measurements were thus carried out in the repulsive regime of TMAFM.[54,55] A phase contrast between PS and PB is obtained because these materials have distinctly different viscoelastic properties at room temperature (PS is a glass, PB a rubber). It is thus possible to discriminate between PS and PB; however, it is not straightforward to relate the magnitude of the phase lag to the material present at the surface.[55] Note also that the absolute value of the phase lag depends strongly on the parameters chosen. In addition, the output for the phase lag by the present equipment is only exact for low values of the phase lag,[56] and therefore, we chose not to give units in the phase images presented below. The height images may be affected by the fact that materials with different viscoelastic properties are present at the surface, and their detailed shape may thus be distorted. However, the lamellar thickness is reproduced correctly.

The AFM images were analyzed using the Scanning Probe Image Processor (SPIP) software from Image Metrology, Lyngby, Denmark. Images showing a surface texture were analyzed by determining the power spectral density (PSD) of the phase images, i.e., the radial average of the two-dimensional Fourier transform of the image. Lateral repeat distances were obtained from the positions of the peaks in the PSD. For this purpose we used the phase images and not the height images because the latter often show a large-scale waviness, which hampers the determination of the peak position in the PSD. In the phase images, on the other hand, only the material contrast is monitored, leading to better defined peaks in the PSD. Average terrace heights were determined by taking the difference between the peak positions in the height histograms. In both cases peak positions were identified by fitting Lorentz functions to the peaks. We chose Lorentz functions for fitting the PSD peaks, as they have a simple analytical form and are reasonably similar to the observed line shapes.

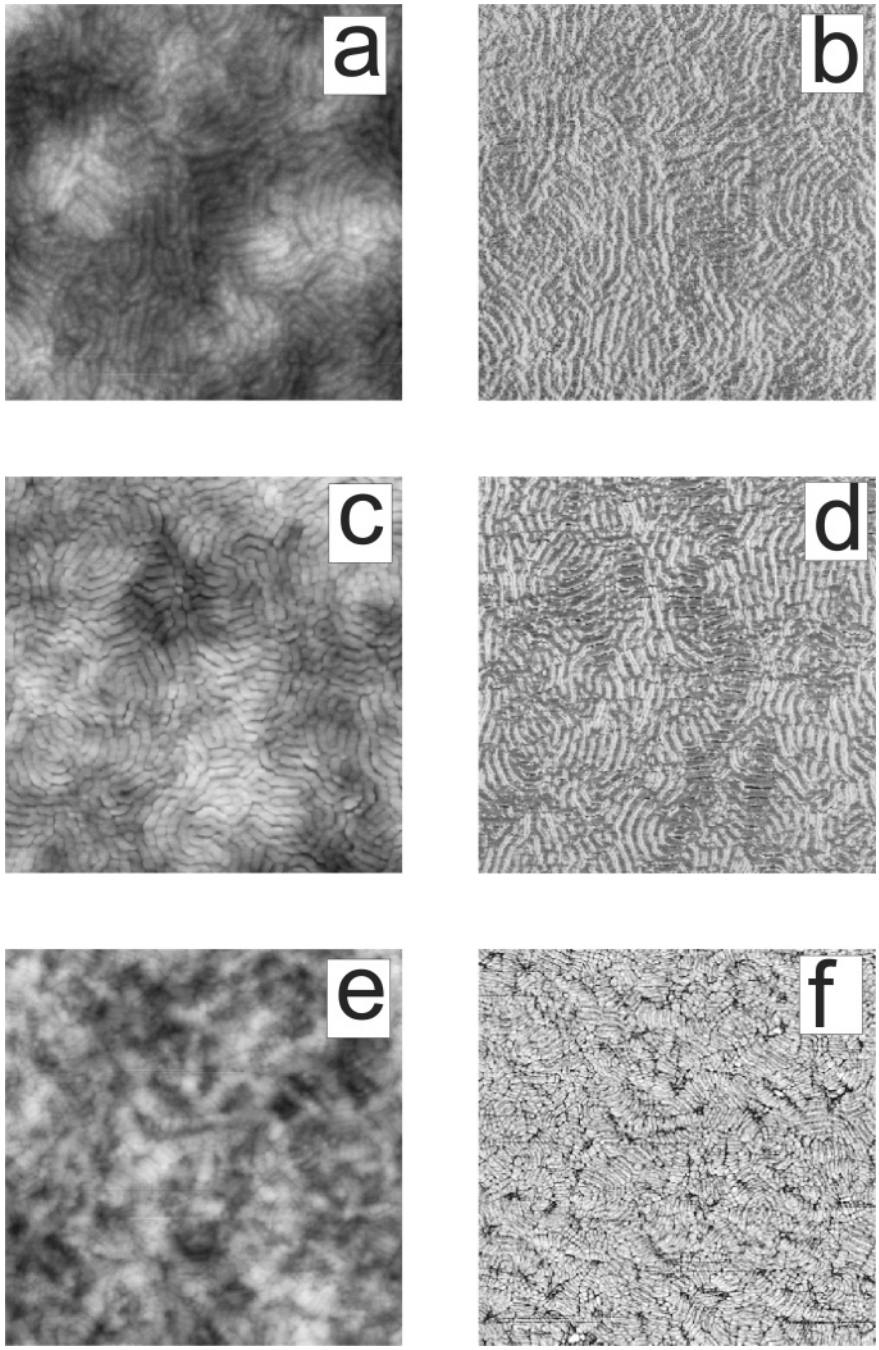

Figure 1. Tapping mode AFM images of spin-coated PS−PB films with high molar mass. Left column: height images; right column: phase images. Image size $3 \times 3\ \mu m^2$. (a, b) $\bar{M}_n = 183$ kg/mol, $D_{red} = 2.8$, scan rate 0.5 Hz, height scale in (a) 200 Å, (c, d) $\bar{M}_n = 148$ kg/mol, $D_{red} = 2.6$, height scale in (c) 200 Å, (e, f) $\bar{M}_n = 91.9$ kg/mol, $D_{red} = 3.2$, height scale in (e) 300 Å.

Results

Molar-Mass Dependence of the Lamellar Orientation in Thin Films with Similar Reduced Film Thicknesses. Figure 1a,b shows the TMAFM height and phase images of a spin-coated film of a high molar mass sample (183 kg/mol, $D_{red} = 2.8 \pm 0.1$) after annealing. In both images, a meandering lamellar texture is observed. The repeat distance of the periodic features was obtained by identifying the position of the peak in the PSD of the phase image (second curve from below in Figure 2). For this sample, a repeat distance of 855 ± 4 Å is obtained, which is in good agreement with the bulk lamellar thickness 839 ± 13 Å,[9,45] determined at 150 °C (Table 1). These observations point to a perpendicular orientation of the lamellae with respect to the film surface. In an earlier cross-section TEM study on lamellar PS−PI samples, where the lamellae are oriented perpendicular to the film surface, a thin layer of PI (the lower surface tension component) was found to cover the sample surface.[24] Similar observations were made by Schwark et al.[25] near the surface of a lamellar PS−PB sample. We were not able to find a clear evidence of such a thin and soft layer with AFM. In case a thin and soft surface layer is present, the phase contrast is expected to vanish at higher set-point ratios (lighter tapping).[54,55] However, not even with set-point ratios higher than our usual value of 0.6 was it possible to detect a thin surface layer in the present work.

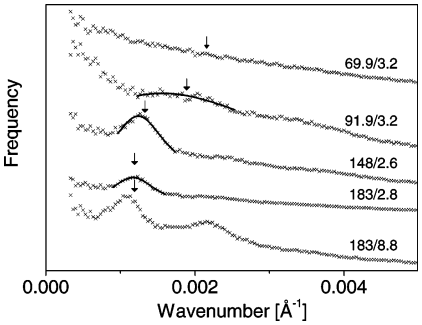

Figure 2. Power spectral densities of the phase images in Figure 1b,d,f and of the phase images corresponding to Figures 3a and 7a. Symbols represent experimental data and lines fits of Lorentz functions. The curves have been shifted vertically for clarity. The arrows mark the wavenumbers expected from D_{lam}. The molar masses in kg/mol and the values of D_{red} are given in the image.

A film with $\bar{M}_n$ = 148 kg/mol and D_{red} = 2.6 ± 0.1 shows a very similar surface texture (Figure 1c,d). The repeat distance, 805 ± 5 Å, obtained from the PSD (middle curve in Figure 2) of the phase image (Figure 1d), is again slightly larger (7%) than the bulk lamellar thickness (752 ± 4 Å, Table 1). The lamellae are thus perpendicular to the film surface as well.

For a sample with 91.9 kg/mol and D_{red} = 3.2 ± 0.1, no well-defined lamellar structure is seen in the surface topography (Figure 1e). However, the phase image (Figure 1f) reveals lamellar grains. The correlation of the lamellar order is, however, only short-ranged compared to the higher molar mass films described above. This is reflected in the broad and flat peak in the PSD (second curve from top in Figure 2). The large width of the peak can be explained by the presence of different lamellar orientations with respect to the surface. In an earlier study, cross-sectional TEM revealed that the lamellae have a tilt angle with respect to the film surface of ∼28° for a PS−PB film of thickness ∼1 mm with nearly identical molar mass.[25] In our case, it cannot completely be excluded that the lamellae are perpendicular to the film surface with a much larger lamellar thickness than in the bulk. However, this would be very unfavorable for copolymers which already are in the strong-segregation limit.[9]

For samples with even lower molar masses, qualitatively different surface structures are observed. Figure 3a shows the height image of a film with 69.9 kg/mol. Neither in the height nor in the phase image (the latter is uniform, not shown) can a lamellar texture be resolved. The PSD does not exhibit a peak (uppermost curve in Figure 2), and it is thus impossible to extract any predominant wavelength. The same block appears to be present at the surface over the entire film, and therefore the height image yields reliable height differences. The surface is wavy on a large length scale (Figure 3b) which is probably caused by a large number of defects. The height histogram of Figure 3b (uppermost curve in Figure 5) shows two overlapping peaks, their maxima being separated by a distance of ∼260 Å.

For even lower molar masses ($\bar{M}_n$ = 18.3−54.5 kg/mol and D_{red} = 2.1−3.2) two dominating height levels can be discerned (Figure 4). This is reflected in the two maxima in the corresponding height histograms in Figure 5. The maxima are relatively narrow for $\bar{M}_n \leq$ 22.6 kg/mol, whereas they are much broader for 54.5 kg/mol. Thus, for $\bar{M}_n \leq$ 54.5 kg/mol, well-defined terraces are present at the surface.

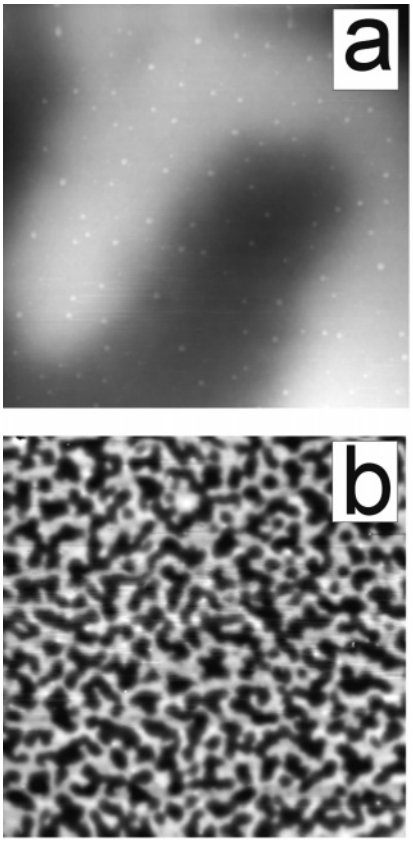

Figure 3. TMAFM height images of spin-coated PS−PB films with $\bar{M}_n$ = 69.9 kg/mol and D_{red} = 3.2: (a) image size 3 × 3 μm^2, height scale 600 Å; (b) image size 50 × 50 μm^2, height scale 500 Å.

The occurrence of terraces with values close or equal to D_{lam} is characteristic for a parallel lamellar orientation in thin, substrate-supported films:[12,16−20] The incommensurability between D_{film} and D_{lam} leads to the formation of an incomplete top layer with a height similar to the bulk lamellar thickness. Comparison of the values of the terrace heights with the bulk lamellar thicknesses at 150 °C (Figure 6) shows that the terrace heights are similar to the D_{lam} values but consistently lower. Comparison of the values of the terrace heights with the bulk lamellar thicknesses at 150 °C (Figure 6) shows that the terrace heights are similar to the D_{lam} values but consistently lower. This seems contradictory because at room temperature D_{lam} would have been expected to be thicker by ∼10%, because the phase separation is stronger and thus the chains are stretched more strongly. The agreement between the terrace heights and D_{lam} is best for the lowest molar masses ($\bar{M}_n \leq$ 22.6 kg/mol), namely 11−19%. This is consistent with a nearly perfect parallel orientation of the lamellae with respect to the film interfaces, with a low defect density inside the film. For samples with $\bar{M}_n$ of 54.5 and 69.9 kg/mol, the deviation between the terrace heights and D_{lam} is larger (>25%). This points to a preferentially parallel orientation of the lamellae in the film with a number of defects, e.g., nonparallel lamellae. This affects the average terrace height and is the more pronounced, the higher the molar mass. To confirm this hypothesis, we investigated the inner structure of the films using GISAXS .[43,57,58] The results obtained are in good agreement with the interpretation of our AFM results.

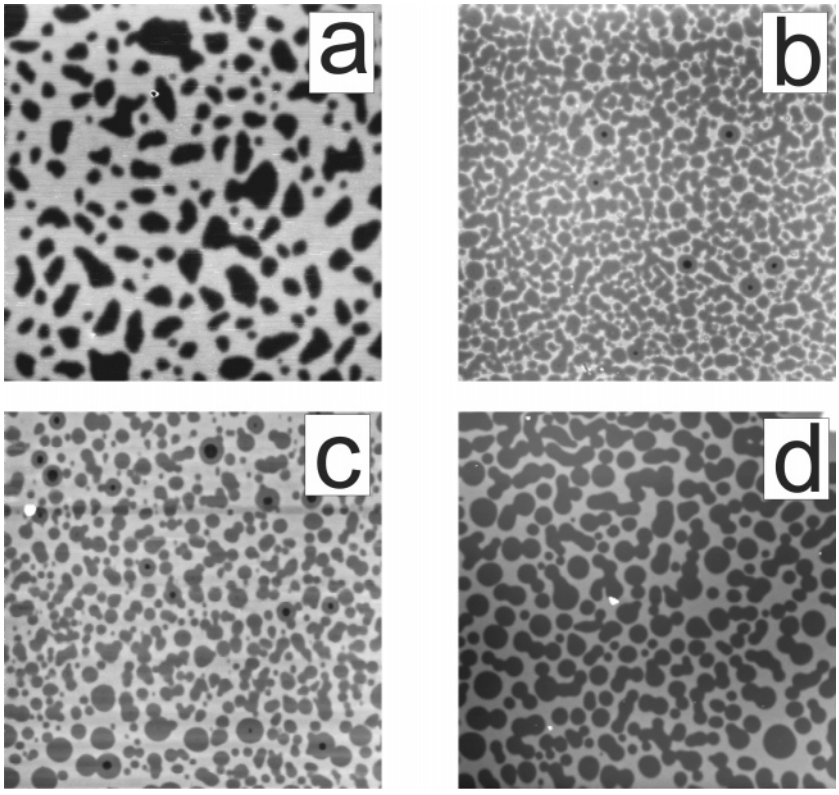

Figure 4. TMAFM height images of low molar mass spin-coated PS−PB films: (a) $\bar{M}_n = 54.5$ kg/mol, $D_{red} = 3.1$, image size 40 × 40 μm^2; (b) $\bar{M}_n = 22.6$ kg/mol, $D_{red} = 2.1$, image size 50 × 50 μm^2; (c) $\bar{M}_n = 22.1$ kg/mol, $D_{red} = 2.4$, image size 50 × 50 μm^2; (d) $\bar{M}_n = 18.3$ kg/mol, $D_{red} = 2.4$, image size 40 × 40 μm^2. Height scale 500 Å in all images.

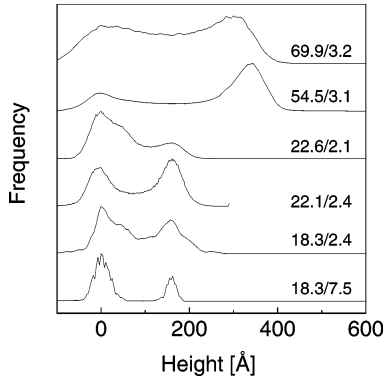

Figure 5. Height histograms of the images in Figure 3b, 4, and 8b. The curves have been shifted vertically for clarity. The molar masses in kg/mol as well as the reduced film thicknesses are indicated in the image.

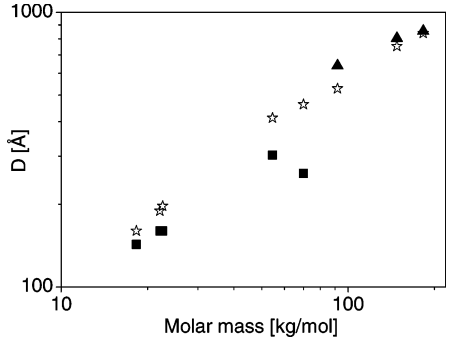

Figure 6. Double-logarithmic representation of the terrace heights (squares) and the lateral repeat distances (triangles) from the films presented in Figures 1, 3, and 4 ($D_{red} = 2.1-3.2$) measured by TMAFM and bulk lamellar thicknesses, D_{lam}, from refs 9 and 45 (stars). The error bars are smaller than the symbol size.

Films with Large Reduced Thickness. The previous section described the orientation of lamellae in films with film thicknesses of a few times the lamellar thickness. For such thin films, it has been predicted that the effect of the confining geometry has a strong influence on the lamellar orientation (between hard walls), whereas for thicker films only the parallel orientation is stable.[30,34] To test the latter prediction, we have prepared both a high ($\bar{M}_n = 183$ kg/mol) and a low ($\bar{M}_n = 22.6$ kg/mol) molar mass sample with large reduced film thicknesses ($D_{red} = 8.0-8.8$). Similar surface textures as for lower D_{red} were observed (Figure 7). For the high molar mass sample (Figure 7a), the lamellar thickness extracted from the PSD (lowermost curve in Figure 2) of the phase image is 923 ± 8 Å, thus 10% higher than D_{lam}. Even a second-order peak can be revealed from the PSD; i.e., the perpendicular lamellar order is well-established. For the low molar mass sample (Figure 7b) the terrace height of 171 ± 1 Å is only 13% smaller than the bulk lamellar thickness. Note that the shape of the holes in Figure 7b resembles the patterns observed in thin films of polystyrene−poly(vinylpyridine) diblock copolymers:[59] There are holes in the uppermost (incomplete) lamellar layer on top of the underlying (complete) film. We conclude that the parallel and the perpendicular orientation of the lamellae at the film surface are not limited to thin films with only a few times the lamellar thickness and are therefore not caused by the confining thin film geometry alone.

Influence of Preparation Method. In several studies, it was shown that the orientation of PS−PB block copolymers near a free film surface depends on the evaporation time of the solvent.[26−28] Furthermore, even though the spin-coating process is a convenient way to produce extended films with very low surface roughness,

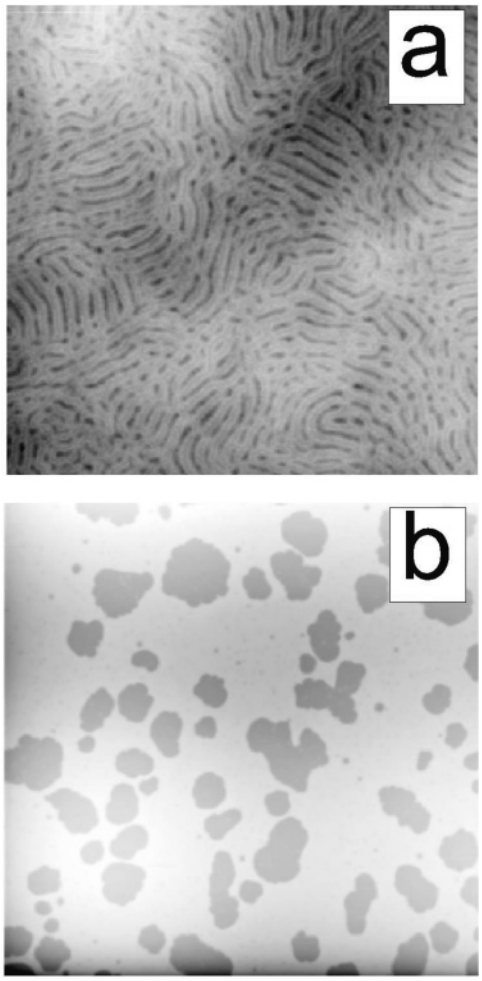

Figure 7. TMAFM height images of thicker spin-coated PS−PB films: (a) $\bar{M}_n = 183$ kg/mol, $D_{red} = 8.8$, image size 3×3 μm^2, height scale 400 Å; (b) $\bar{M}_n = 22.6$ kg/mol, $D_{red} = 8.0$, image size 100×100 μm^2, height scale 1200 Å.

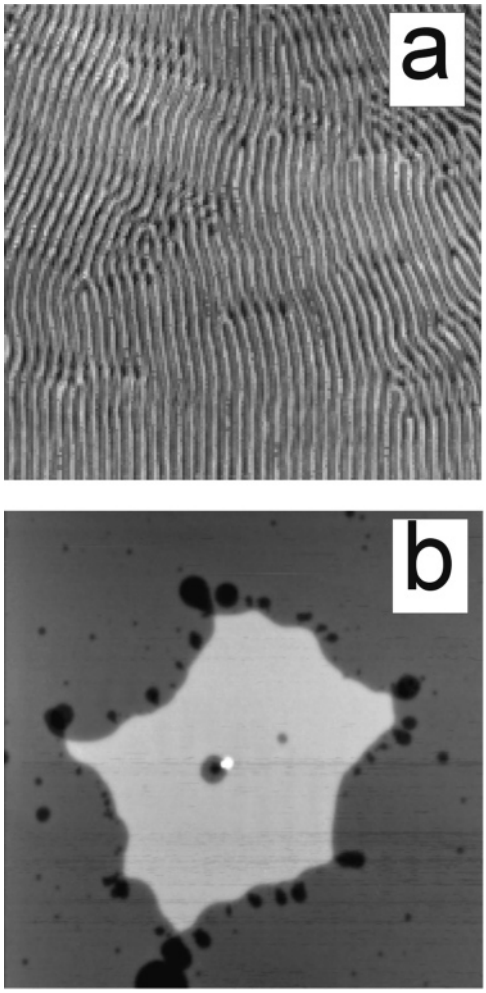

Figure 8. TMAFM height images of slowly solvent-cast PS−PB films: (a) $\bar{M}_n = 183$ kg/mol and $D_{red} \approx 2$. Image size 3×3 μm^2, height scale 100 Å. (b) $\bar{M}_n = 18.3$ kg/mol, $D_{red} \approx 7.5$. Image size 30×30 μm^2, height scale 400 Å.

it is also a rather fast process and may lead to nonequilibrium structures. To clarify this point, two samples were prepared by slow solvent-casting as described in the Experimental Section. The film thicknesses were inhomogeneous: $D_{red} \approx 2.0-5.0$ for a sample with 183 kg/mol and 1.5−7.5 for 18.3 kg/mol. Independent of the local film thickness, these films show surface textures which are qualitatively identical to those of the spin-coated films of identical molar mass (Figures 1a,b and 4d).

The high molar mass film shows a meandering lamellar surface texture (Figure 8a). At the position where the image was recorded, the local reduced film thickness is $D_{red} \approx 2$. The repeat distance of the lamellae observed (771 ± 4 Å) is close to D_{lam}. Comparison of the surface textures of the spin-coated (Figures 1a,b) and the solvent-cast film (Figure 8a) shows that the latter has a lower defect density. This is also reflected in lower magnification images (not shown here).

The surface of the solvent-cast low molar mass film ($D_{red} \approx 7.5$) shows terraces (Figure 8b) and no lateral structuring on the length scale of the lamellar thickness. The terrace height of this sample as extracted from the height histogram, lowermost curve in Figure 5, is 158 ± 1 Å, i.e., in very good agreement with $D_{lam} = 160 \pm 3$ Å. The film thus consists of a layer of seven lamellae covering the substrate. On top, an incomplete layer dewets from the underlying layer, which gives rise to the plateau in Figure 8b, similar to the observations made in ref 59. The dark spots appear to be holes with a height difference of $\sim 2D_{lam}$ with respect to the plateau in the middle of the image. The parallel lamellar orientation is thus formed during both spin-coating and solvent-casting.

Hence, a change of the solvent evaporation time from a few seconds (spin-coating) to a few days (solvent-casting) leads to the same lamellar orientation. Even though it cannot be confirmed unequivocally that an equilibrium state is attained, both the parallel orientation for low molar mass samples and the perpendicular orientation for high molar mass samples are reproducible and are independent of the preparation route.

Films with Thicknesses Similar to or Lower than the Bulk Lamellar Thickness. Most spin-coated samples with film thicknesses $D_{red} \approx 1$ do not show any characteristic surface texture. One example is given in Figure 9, where a height and a phase image of a film with $\bar{M}_n = 54.5$ kg/mol and $D_{red} = 0.9$ are shown. In contrast to the thicker film shown in Figure 4a, no terraces are observed, but the surfaces are flat and homogeneous. This is consistent with symmetric wetting; i.e., the same block tends to adsorb at both interfaces. As PB has a lower surface tension than PS (28 and 33 mN/m, respectively[26]), we conclude that the free film surface is covered by PB. The film thus consists of PB layers with thicknesses of about $D_{lam}/4$ at both

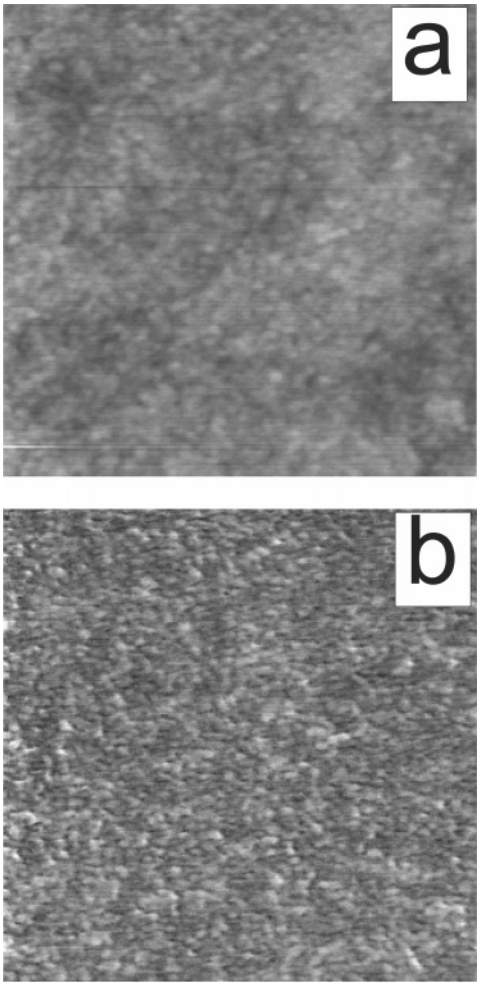

Figure 9. TMAFM height (a) and phase image (b) of spin-coated, ultrathin PS−PB films. Image size 3 × 3 μm^2. $\bar{M}_n$ = 54.5 kg/mol, D_{red} = 0.9. Height scale in (a) 50 Å.

the substrate and the free film surface and a PS layer of thickness of about $D_{lam}/2$ in between.

In contrast, for films with $D_{red} \approx 0.5$, both high and intermediate molar mass films (183 and 54.5 kg/mol) show a weakly structured surface topography, which points to a perpendicular orientation at the film surface (Figure 10). As for thicker films, this surface structuring is again stronger for higher molar masses (Figure 10c,d). According to the theoretical predictions for ultrathin films,[10] this observation is also consistent with symmetric wetting. It is not possible to judge, though, whether the structures observed for $D_{red} \approx 0.5$ are due to the perpendicular lamellar orientation or to the hybrid morphologies described in ref 10 because their surface topographies are expected to be very similar. Note that symmetric wetting means that the same block is preferentially adsorbed to both film interfaces, but the strength of their selectivity is not necessarily the same.

Discussion

The results of the experiments presented in the last section are compiled in Figure 11. Here, the lamellar orientations encountered are given as a function of the reduced film thickness, D_{red}, and the molar mass ($\bar{M}_n$, bottom) or the bulk lamellar thickness (D_{lam}, top). For low molar mass samples ($\bar{M}_n \leq 22.6$ kg/mol), terraces were observed for nearly all reduced film thicknesses (up triangles). The terrace height is less than 20% smaller than D_{lam}. This difference between the terrace heights and D_{lam} may be caused by a small number of defects within the film which have been detected by GISAXS.[43] Only a few samples did not show any surface structure, which can be explained by a complete top layer. Thus, also for these samples a parallel orientation is plausible. For high molar mass samples ($\bar{M}_n \geq 148$ kg/mol), a surface topography could be observed, which is consistent with lamellae oriented perpendicular to the film surface (down triangles). These findings are independent of D_{red} in the range between unity and ten. For molar masses in between these two regimes, the results are more complex. For $\bar{M}_n$ = 54.5 kg/mol with D_{red} = 3.1, terraces are observed as well, but with a terrace height significantly smaller than D_{lam} (26%). This result is consistent with a parallel orientation of the lamellae, where the parallel order is distorted by a large number of defects. This structure is even more pronounced for a sample with $\bar{M}_n$ = 69.9 kg/mol and D_{red} = 3.2. Here, a wavy surface with a bimodal height distribution was observed, where the difference between the two prominent heights is 43% smaller than D_{lam}. This points to the presence of different orientations (parallel, perpendicular, and tilted) inside the film. For a sample with $\bar{M}_n$ = 91.9 kg/mol, lamellar domains were detected at the free film surface with a broad distribution of lamellar thicknesses. Thus, for this molar mass the interactions responsible for the parallel or the perpendicular orientation (for low and high molar masses, respectively) seem to balance, leading to a mixed orientation. For samples with a reduced film thickness comparable to or less than one, only weakly structured or homogeneous surfaces could be observed.

For PS−PB, the selectivity of the film/air surface (selective for PB) is comparable to the one in PS−PMMA (selective for PS); however, we assume the selectivity of the Si/SiO_x interface toward PB in PS−PB thin films to be much weaker than the selectivity toward PMMA in the PS−PMMA system. The selectivity of the substrate for PB is expected to be weak but not necessarily vanishing. Thus, the enthalpic contribution of the Si/SiO_x interface to the total free energy of the films is less pronounced than for PS−PMMA, and other contributions are likely to become more important.

A model taking into account additional, entropic contributions to the copolymer free energy near a hard wall was suggested by Pickett et al.[35] This model seems to be well-suited to describe the behavior of supported PS−PB films and the difference to PS−PMMA films. Furthermore, the contributions to the free energy are given explicitly as a function of chain length, which allows a tentative explanation of the molar-mass dependence of the lamellar orientation in PS−PB observed by us. Using scaling arguments, the difference in the free energy between the parallel and perpendicular orientation, $\Delta = E_{||} - E_{\perp}$, is expressed by

$$\Delta = \Delta_W + \Delta_n + \Delta_e = \frac{a}{N}[-c_W N^1 + c_n N^{1/3} - c_e N^{1/9}] \quad (1)$$

where Δ_W, Δ_n, and Δ_e are the contributions from surface wetting, nematic ordering of stretched chains at a wall, and the enrichment of free end segments near a film interface, respectively. c_W, c_n, and c_e are constant prefactors, and a and N are the segment length and the copolymer degree of polymerization, respectively.[35] The first term in eq 1 describes the influence of the

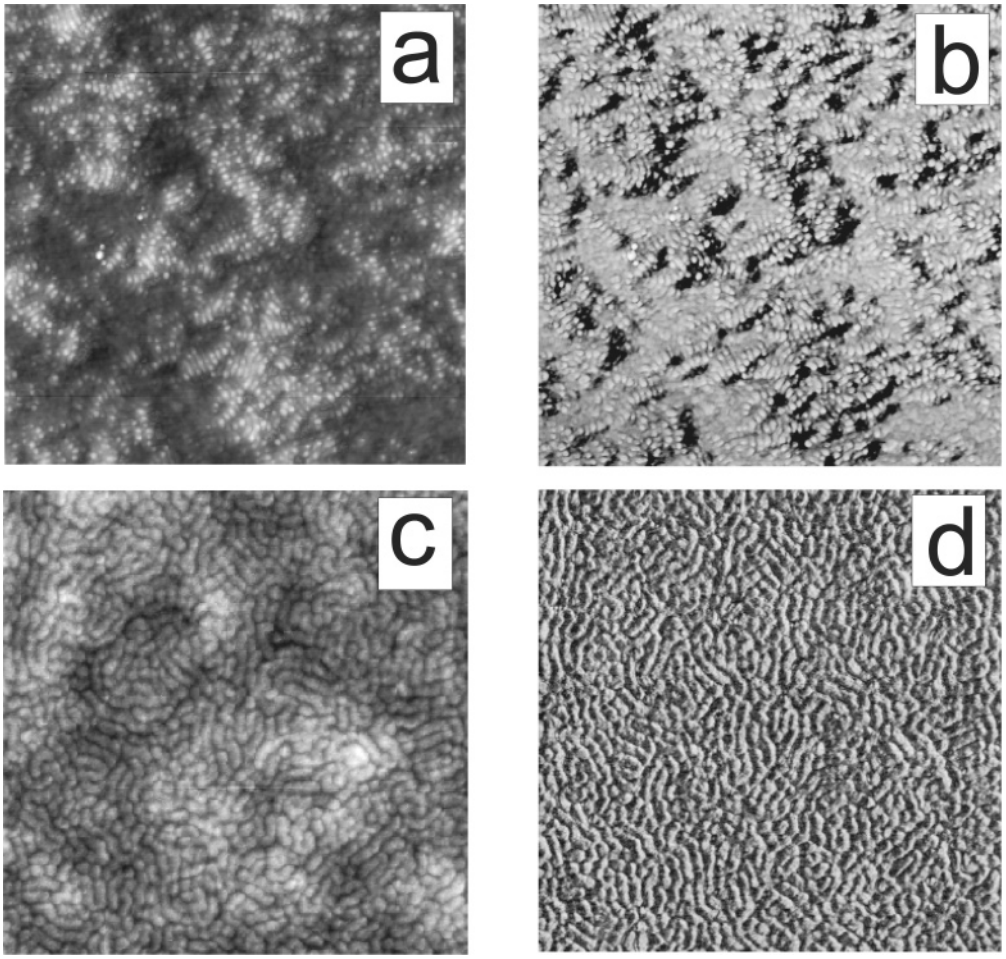

Figure 10. TMAFM height (a, c) and phase images (b, d) of spin-coated, ultrathin PS−PB films. Image size 3 × 3 μm^2. (a, b) $\bar{M}_n$ = 54.5 kg/mol, D_{red} = 0.5; (c, d) M_n = 183 kg/mol, D_{red} = 0.6. The height scale in (a) and (c) is 100 Å.

interfaces present in the film (both blocks A and B with the substrate, with air and at the lamellar interfaces between the two blocks), expressed by their interfacial tensions: $\gamma_{A/sub}$, $\gamma_{B/sub}$, $\gamma_{A/air}$, $\gamma_{B/air}$, and γ_{AB}, where "sub" stands for substrate. It thus describes the selectivity of the wall toward one of the blocks. This contribution has also been considered in other theoretical approaches,[29,30,34] and equivalent expressions were obtained. The nematic term, Δ_n, is related to chain stretching: In the bulk, diblock copolymer chains are stretched normal to the lamellar interfaces, which causes an entropic loss with respect to Gaussian conformation. If these stretched chains come into contact with a hard wall, alignment along the wall stabilizes their stretched conformation, thus lowering the entropic loss.[35,36] The combination of these effects forces the lamellae to orient perpendicular to the film surfaces. The last term, Δ_e, takes into account that the enrichment of free end segments near a wall lowers the interfacial tension because of their higher degree of freedom (i.e., higher entropy) compared to the other segments in the chain. As the concentration of chain ends is highest in the center of the lamellar parts (i.e., between two lamellar interfaces), this effect forces the lamellae to orient parallel to the wall.

To compare the consequences of this model to the molar-mass dependence of the lamellar orientation in the PS−PB system, we need to analyze the N dependence of Δ_n and Δ_e for the case of small Δ_W. If Δ_W is sufficiently small, the entropic contributions Δ_n and Δ_e become important. Especially for low molar masses, the chain end effect can dominate the nematic effect, leading to a negative sign of Δ in eq 1 and thus to the parallel orientation. As this contribution decays much more rapidly with increasing N than the nematic term, a crossover is expected, where Δ becomes positive and the perpendicular orientation becomes stable. The latter would be the case for high molar mass. Only for extremely high molar masses a parallel orientation again becomes possible. The model thus can describe the behavior observed in supported PS−PB films.

The transition between these two limiting cases (parallel lamellae for low N and perpendicular lamellae for high N) depends on the values of the prefactors c_n and c_e which, in turn, depend on material parameters that are difficult to obtain. A quantitative analysis of eq 1 would require the knowledge of parameters which are not accessible to us, e.g., $\gamma_{PS/sub}$ and $\gamma_{PB/sub}$, and the concentration profile of free chain ends along the lamellar normal. Thus, we can only discuss the above model qualitatively.

To explain the difference between the PS−PB and PS−PMMA, we note once more that the interfacial tension between the polar PMMA and Si/SiO_x is presumably much lower than the one between PB and Si/SiO_x because PB is rather nonpolar. Therefore, Δ_W in PS−PMMA is assumed to be larger than in PS−PB. For large values of Δ_W, the parallel orientation is favored for any value of N. This has been observed frequently with PS−PMMA on Si/SiO_x substrates.

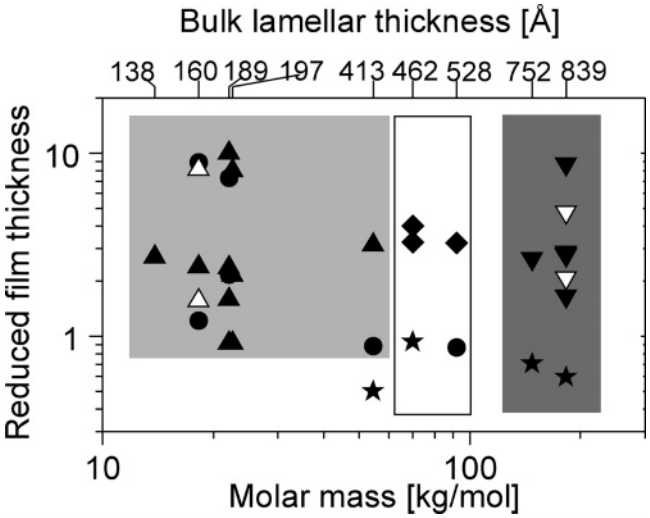

Figure 11. Lamellar orientation at the free film surface as a function of the reduced film thickness and molar mass. The top axis gives the D_{lam} values from refs 9 and 45. Filled symbols: spin-coated samples; open symbols: solvent-cast samples. Triangles up: terraces; triangles down: lamellar texture; diamonds: coexisting orientations; stars: weak surface texture; circles: no surface texture. The shaded regions indicate the orientations identified. Light gray: predominantly parallel orientation; dark gray: predominantly perpendicular orientation; white: coexistence of different orientations.

These observations relate to the interaction between the diblock copolymer film and the substrate. However, we need to consider the other interfaces in the film as well in order to explain the different behavior of PS−PB and PS−PMMA. The difference in surface tension between the two blocks with respect to air, $\gamma_{A/air} - \gamma_{B/air}$, is of the same order of magnitude for both PS−PB and PS−PMMA, namely about 5 mN/m.[47−49] The tension of the lamellar interfaces γ_{AB} is related to the Flory−Huggins interaction parameter χ by $\gamma_{A/B} \propto \sqrt{\chi}/6$.[3] For PS−PB, this value is significantly higher than for PS−PMMA:[60] At room temperature, $\chi \simeq 0.09$ for PS−PB[45] and ∼0.04 for PS−PMMA.

The latter observation can explain why the lamellae are parallel or perpendicular not only at the film/substrate interface but throughout the film and up to the film surface, even though the nematic effect is a surface-induced effect and hence of very short range (a few nanometers at most). We have evidence from complementary studies on the same films with GISAXS that the perpendicular orientation can persist over a distance of at least $2-3D_{lam}$.[43] We ascribe the large distance over which the perpendicular orientation is stable to the high interfacial tension of PS−PB. A reorientation of the lamellar interface within the film would result in a high energy cost, and therefore, the perpendicular orientation induced by the substrate is stable over a longer range than would be expected from the strength of the nematic effect alone. For PS−PMMA, the perpendicular lamellar orientation close to a non-selective film interface persists only over a short range,[41] possibly because of the relatively low χ parameter of PS−PMMA.[21]

Conclusion

Our tapping mode atomic force microscopy study of lamellar diblock copolymer thin films showed that, for blocks that interact only weakly with the substrate surface and with air, molar mass is the key factor for the lamellar orientation in spin-coated thin films. Whereas for high molar mass PS−PB copolymers ($\bar{M}_n$ = 91.9−183 kg/mol) a perpendicular orientation of the lamellae with respect to the free film surface is observed, the lamellae in low molar mass samples ($\bar{M}_n$ = 13.9−54.4 kg/mol) align preferentially parallel to the surface. Films with film thicknesses close to D_{lam} do not show any surface texture, whereas films with film thicknesses close to one-half of the lamellar thickness have weakly textured surfaces. These observations point to symmetric wetting; i.e., both interfaces slightly favor the PB block. Solvent-casting leads to the same lamellar orientations as spin-coating.

We suggest an explanation of our findings based on a theoretical model by Pickett et al. We conclude that in the PS−PB system the enthalpic contributions to the interfacial energies do not favor one of the blocks strongly and that entropic contributions such as the nematic effect and the chain end effect are of equal importance. Because of the different scaling behavior of these contributions with the chain lengths, high molar mass samples seem to favor the perpendicular lamellar orientation, while we find weakly ordered parallel lamellae for the short chains.

Acknowledgment. The authors thank Prof. I. I. Potemkin for stimulating discussions and Dr. A. Khaidarov for help with the solvent-casting experiments. Financial support by DFG, NATO, and Fonds der Chemischen Industrie is gratefully acknowledged.

References and Notes

(1) Spatz, J. P.; Eibeck, P.; Mössmer, S.; Möller, M.; Herzog, T.; Ziemann, P. *Adv. Mater.* **1998**, *10*, 849.
(2) Thurn-Albrecht, T.; Steiner, R.; DeRouchey, J.; Stafford, C. M.; Huang, E.; Bal, M.; Tuominen, M.; Hawker, C. J.; Russell, T. P. *Adv. Mater.* **2000**, *12*, 787.
(3) Bates, F. S.; Fredrickson, G. H. *Annu. Rev. Phys. Chem.* **1990**, *41* 525.
(4) Khandpur, A. K.; Förster, S.; Bates, F. S.; Hamley, I. W.; Ryan, A. J.; Bras, W.; Almdal, K.; Mortensen, K. *Macromolecules* **1995**, *28*, 8796.
(5) Hamley, I. W. *The Physics of Block Copolymers;* Oxford University Press: Oxford, 1998 and references therein.
(6) Bartels, V. T.; Stamm, M.; Abetz, V.; Mortensen, K. *Europhys. Lett.* **1995**, *31* 81.
(7) Helfand, E.; Wasserman, Z. R. *Macromolecules* **1976**, *9*, 879.
(8) Semenov, A. N. *Sov. Phys. JETP* **1985**, *61*, 733; *Zh. Eksp. Teor. Fiz.* **1985**, *88*, 1242.
(9) Papadakis, C. M.; Almdal, K.; Mortensen, K.; Posselt, D. *Europhys. Lett.* **1996**, *36*, 289.
(10) Fasolka, M. J.; Mayes, A. M. *Annu. Rev. Mater. Res.* **2001**, *31*, 323.
(11) Anastasiadis, S. H.; Russell, T. P.; Satija, S. K.; Majkrzak, C. F. *Phys. Rev. Lett.* **1989**, *62*, 1852.
(12) Coulon, G.; Ausserré, D.; Russell, T. P. *J. Phys. (Paris)* **1990**, *51*, 777.
(13) Krausch, G. *Mater. Sci. Eng.* **1995**, *R14*, 1 and references therein.
(14) Mansky, P.; Russell, T. P.; Hawker, C. J.; Mays, J.; Cook, D. C.; Satija, S. K. *Phys. Rev. Lett.* **1997**, *79*, 237.
(15) Mansky, P.; Russell, T. P.; Hawker, C. J.; Pitsikalis, M.; Mays, J. *Macromolecules* **1997**, *30*, 6810.
(16) Coulon, G.; Collin, B.; Ausserré, D.; Chatenay, D.; Russell, T. P. *J. Phys. (Paris)* **1990**, *51*, 2801.
(17) Ausserré, D.; Chatenay, D.; Coulon, G.; Collin, B. *J. Phys. (Paris)* **1990**, *51*, 2571.
(18) Maaloum, M.; Ausserré, D.; Chatenay, D.; Coulon, G.; Gallot, Y. *Phys. Rev. Lett.* **1992**, *68*, 1575.
(19) Cai, Z. H.; Huang, K.; Montano, P. A.; Russell, T. P.; Bai, J. M.; Zajak, G. W. *J. Chem. Phys.* **1993**, *98*, 2376.
(20) Cai, Z. H.; Lai, B.; Yun, W. B.; McNulty, I.; Huang, K. G.; Russell, T. P. *Phys. Rev. Lett.* **1994**, *73*, 82.
(21) Menelle, A.; Russell, T. P.; Anastasiadis, S. H.; Satija, S. K.; Majkrzak, C. F. *Phys. Rev. Lett.* **1992**, *68*, 67.

(22) Fredrickson, G. H. *Macromolecules* **1987**, *20*, 2535.
(23) Lambooy, P.; Russell, T. P.; Kellogg, G. J.; Mayes, A. M.; Gallagher, P. D.; Satija, S. K. *Phys. Rev. Lett.* **1994**, *72*, 2899.
(24) Hasegawa, H.; Hashimoto, T. *Macromolecules* **1985**, *18*, 589.
(25) Schwark, D. W.; Vezie, D. L.; Reffner, J. R.; Thomas, E. L. *J. Mater. Sci. Lett.* **1992**, *11*, 352.
(26) Turturro, A.; Gattiglia, E.; Vacca, P.; Viola, G. T. *Polymer* **1995**, *36*, 3987.
(27) Kim, G.; Libera, M. *Macromolecules* **1998**, *31*, 2569.
(28) Kim, G.; Libera, M. *Macromolecules* **1998**, *31*, 2670.
(29) Turner, M. S. *Phys. Rev. Lett.* **1992**, *69*, 1788.
(30) Walton, D. G.; Kellogg, G. J.; Mayes, A. M.; Lambooy, P.; Russell, T. P. *Macromolecules* **1994**, *27*, 6225.
(31) Matsen, M. W. *J. Chem. Phys.* **1997**, *106*, 7781.
(32) Tang, W. H.; Witten, T. A. *Macromolecules* **1998**, *31*, 3130.
(33) Tsori, Y.; Andelmann, D. *Eur. Phys. J. E* **2001**, *5*, 605.
(34) Geisinger, T.; Müller, M.; Binder, K. *J. Chem. Phys.* **1999**, *111*, 5241, 5251.
(35) Pickett, G. T.; Witten, T. A.; Nagel, S. R. *Macromolecules* **1993**, *26*, 3194.
(36) Pickett, G. T.; Balazs, A. C. *Macromolecules* **1997**, *30*, 3097.
(37) Sommer, J.-U.; Hoffmann, A.; Blumen, A. *J. Chem. Phys.* **1999**, *111*, 3728.
(38) Kellogg, G. J.; Walton, D. G.; Mayes, A. M.; Lambooy, P.; Russell, T. P.; Gallagher, P. D.; Satija, S. K. *Phys. Rev. Lett.* **1996**, *76*, 2503.
(39) Huang, E.; Rockford, L.; Russell, T. P.; Hawker, C. J. *Nature (London)* **1998**, *395*, 757.
(40) Huang, E.; Pruzinsky, S.; Russell, T. P.; Mays, J.; Hawker, C. J. *Macromolecules* **1999**, *32*, 5299.
(41) Huang, E.; Mansky, P.; Russell, T. P.; Harrisson, C.; Chaikin, P. M.; Register, R. A.; Hawker, C. J.; Mays, J. *Macromolecules* **2000**, *33*, 80.
(42) Fasolka, M. J.; Banerjee, P.; Mayes, A. M.; Pickett, G.; Balazs, A. C. *Macromolecules* **2000**, *33*, 5702.
(43) Busch, P.; Posselt, D.; Smilgies, D.-M.; Rauscher, M.; Papadakis, C. M. Manuscript in preparation.
(44) Ndoni, S.; Papadakis, C. M.; Bates, F. S.; Almdal, K. *Rev. Sci. Instrum.* **1995**, *66*, 1090.
(45) Papadakis, C. M.; Almdal, K.; Mortensen, K.; Posselt, D. *J. Phys. II* **1997**, *7*, 1829.
(46) Rudd, J. F. In *Polymer Handbook*, 3rd ed.; Brandrup, J., Immergut, E. H., Eds.; Wiley: New York, 1989.
(47) Shafrin, E. G. In *Polymer Handbook*, 2nd ed.; Brandrup, J., Immergut, E. H., Eds.; Wiley: New York, 1975.
(48) Wu, S. In *Polymer Handbook*, 3rd ed.; Brandrup, J., Immergut, E. H., Eds.; Wiley: New York, 1989.
(49) Owen, J. O. In *Physical Properties of Polymers Handbook;* Mark, J. E., Ed.; AIP Press: Woodbury: NY, 1996.
(50) Shibayama, M.; Hashimoto, T.; Hasegawa, H.; Kawai, H. *Macromolecules* **1983**, *16*, 1427.
(51) Leonard, D. N.; Russell, P. E.; Smith, S. D.; Spontak, R. J. *Macromol. Rapid Commun.* **2002**, *23*, 205.
(52) Azzam, R. M. A.; Bashara, N. M. *Ellipsometry and Polarized Light;* North-Holland: Amsterdam, 1984.
(53) Bartels, J.; Borchers, H.; Hausen, H.; Hellwege, K. H.; Schäfer, K. L.; Schmidt, E. *Landolt-Börnstein Zahlenwerte und Funktionen*, 6th ed.; Springer-Verlag: Berlin, 1962; Vol. II, Part 8.
(54) Magonov, S. N.; Cleveland, J.; Elings, V.; Denley, D.; Whangbo, M. H. *Surf. Sci.* **1997**, *389*, 201.
(55) Knoll, A.; Magerle, R.; Krausch, G. *Macromolecules* **2001**, *34*, 4159.
(56) http://spm.di.com/archives/m/2001/05/20010509.txt/2.html.
(57) Smilgies, D.-M.; Busch, P.; Papadakis, C. M.; Posselt, D. *Synchrotron Radiat. News* **2002**, *15*, 35.
(58) Busch, P.; Posselt, D.; Smilgies, D.-M.; Kremer, F.; Papadakis, C. M. *Makromol. Chem. Phys.* **2003**, *204*, F18.
(59) Koneripalli, N.; Bates, F. S.; Fredrickson, G. H. *Phys. Rev. Lett.* **1998**, *81*, 1861.
(60) Balsara, N. P. In *Physical Properties of Polymers Handbook;* Mark, J. E., Ed.; AIP Press: Woodbury, NY, 1996.

MA034375R